Available online at www.sciencedirect.com
ScienceDirect
Trans. Nonferrous Met. Soc. China 28(2018) 1611−1617
Transactions of Nonferrous Metals Society of China
www.tnmsc.cn

Tunable emission of cadmium-free transition metal (Cu, Mn, Ag) co-doped ZnInS/ZnS core-shell quantum dots

Qiu-hang CHEN, Shi-liang MEI, Wu YANG, Wan-lu ZHANG, Gui-lin ZHANG, Jia-tao ZHU, Rui-qian GUO

Institute for Electric Light Sources, Engineering Research Center of Advanced Lighting Technology, Ministry of Education, Fudan University, Shanghai 200433, China

Received 16 April 2017; accepted 18 September 2017

Abstract: Color tunable quantum dots (QDs) based on the Cu, Mn, Ag co-doped ZnInS core and ZnS outer-shell were synthesized by using an eco-friendly method. Core-shell doped QDs with the average size of 3.85 nm were obtained by using a one-pot synthesis followed by a hot injection with *n*-dodecanethiol (DDT) and oleylamine (OLA) as stabilizers in oil phase. Cu, Mn and Ag ions were introduced as single-dopant or co-dopants during the synthesis, providing an effective means to control the emission color of the QDs. The as-synthesized QDs showed photoluminescence emission ranging from green (530 nm) to near-red (613 nm), adjusted by doping components, dopant concentration, and Zn/In ratio. Importantly, quasi-white emission has been achieved by controlling the concentration of co-doped metal ions (Mn, Cu and Ag). The primary results demonstrated the promising potential of co-doped QDs as alternative materials for future high quality white LED applications.

Key words: zinc group quantum dots; core-shell; doping; tunable emission; white light

1 Introduction

Semiconductor nanocrystals (quantum dots, QDs) have attracted much attention in display and lighting fields, for their unique optical characteristics such as the size-tunable optical properties and narrow emission spectrum [1−4]. Though CdSe [5], CdTe [6] and PbS [7] QDs have been extensively investigated, the toxicity of heavy metals, such as Cd and Pb, in the QDs limits their applications. Among various inorganic QDs, zinc chalcogenide-based QDs have been a class of the main components for lighting materials [8,9]. Zinc chalcogenides have the advantages of wide bandgap, low toxicity (cadmium-free), and easy synthesis with availability of metal-ion doping [10,11]. For example, Mn-doped ZnS and Mn, Cu-doped ZnSe for tunable or white light emission [12].

II−III−VI ternary QDs with tunable host bandgaps, such as Zn−In−S QDs, are considered low-toxicity alternatives for applications as color-tunable emitters. Different from II−VI QDs, the bandgap of ternary host QD materials depends not only on the composition, but also the size of the intrinsic QDs. Recently, studies on introducing doping metal-ions into Zn−In−S QDs system have achieved much success [13−20]. For example, PRADHAN [21] reported Mn-doped Zn−Cu−In−S and Zn−Ag−In−S QDs with doped emission. The effect of the dopant positions inside core-shell QDs or host compositions on the optical properties of doped core-shell ternary QDs has been explained [22,23]. However, the interaction of multi-doped metal-ions still lacks answers.

In this study, we used ZnInS/ZnS core-shell QDs as model systems to investigate the optical properties of (Cu, Mn, Ag) single-doped or co-doped QDs and the interaction of doping metal-ions. We show a facile synthesis of QDs with ZnInS core, doped with Mn (Cu, Ag), and ZnS shell, and an easy control of their emission wavelength by adjusting dopant composition and concentration of doping ions.

2 Experimental

2.1 Materials

Zinc acetate ($Zn(AcO)_2$, 99.0%), indium sulfate ($In_2(SO_4)_3$, 99.7%), copper chloride ($CuCl_2$, 99.7%), silver nitrate ($AgNO_3$, 99.9%), manganese acetate

Foundation item: Projects (61675049, 61377046, 61144010, 61177021) supported by the National Natural Science Foundation of China
Corresponding author: Rui-qian GUO; Tel: +86-21-55664588; E-mail: rqguo@fudan.edu.cn
DOI: 10.1016/S1003-6326(18)64803-4

($Mn(AcO)_2$, 95.0%), *n*-dodecanethiol (DDT, 98%), oleic acid (OA, 98%), sulfur powder (S, 99.5%), oleylamine (OLA, 80%−90%) and 1-octadecene (ODE, 90%) were purchased from Aladdin. All chemicals were used without further purification.

2.2 Preparation of single-doped and co-doped ZnInS/ZnS core-shell QDs

In a typical reaction (e.g., Mn, Ag co-doped ZnInS/ZnS core-shell QDs), 1.6 mmol of sulfur powder, 0.05 mmol of $CuCl_2$, 0.05 mmol of $AgNO_3$, 0.05 mmol of $Mn(AcO)_2$, 0.5 mmol of $Zn(AcO)_2$, 0.25 mmol of $In_2(SO_4)_3$, 4 mL of DDT and 6 mL of OLA were loaded in 50 mL three-neck flask and degassed twice for 10 min. The mixture was heated to 90 °C and then it was degassed again for 10 min. The mixture was heated to 200 °C with stirring. Growth was continued at 200 °C for 1 h. The ZnS shell formation steps were conducted without intermediate purification. To do this, 1 mL of Zn precursor solution was injected rapidly, and the injection was repeated three times with an interval of 15 min. The solution was cooled down to room temperature.

To obtain the single-doped and co-doped ZnInS QDs, the amount of the dopant precursors was varied while the gross amount of the Zn and In precursors and all other variables remained constant. The concentration of the dopants (X) is represented by the nominal X/(Zn+In) precursor molar ratio.

2.3 Characterization

The resulting QDs were purified by first dissolving in hexane/methanol and precipitating out with acetone, centrifuging, and then re-dispersing in hexane. Purified QDs were dispersed in hexane for UV−Vis absorption spectroscopy (UV−Vis), photoluminescence (PL) spectroscopy, and transmission electron microscopy (TEM) measurements. The absorption and fluorescence spectra were recorded at room temperature on a Shimadzu UV−3600 ultraviolet spectrophotometer and a Shimadzu RF−5301PC fluorescence spectrophotometer, respectively. TEM and high-resolution TEM (HRTEM) images were obtained on JEM−2100F HRTEM. The PL quantum yield (QY) was calculated by using the relative quantum efficiency of the QDs compared with the reference of Rhodamine 6G (QY=95% in ethanol), using the following equation [24]:

$$Q = Q_{\text{std}} \times \frac{I}{I_{\text{std}}} \times \frac{A_{\text{std}}}{A} \times \left(\frac{n}{n_{\text{std}}} \right)^2 \quad (1)$$

where Q and Q_{std} represent the PL QY and the standard (Rhodamine 6G) for these QDs, respectively; I and I_{std} are the measured integrated PL emission intensity at a specified wavelength, respectively; A and A_{std} are the absorbance intensities and the standard of the QDs at the same wavelength for excitation, respectively; n and n_{std} are the refractive indices and the standard of the QDs of the solvents, respectively.

3 Results and discussion

3.1 Cu-doped ZnInS/ZnS core-shell QDs

Figure 1 shows the typical TEM and HRTEM images of Cu-doped ZnInS/ZnS (Cu:ZnInS/ZnS) QDs.

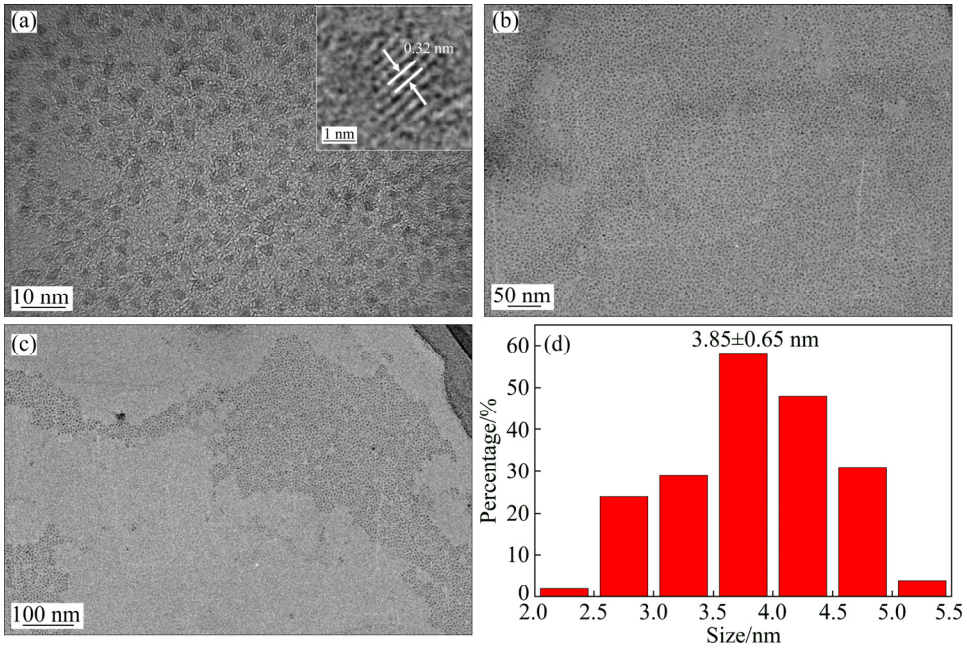

Fig. 1 HRTEM images of Cu:ZnInS/ZnS QDs with Cu concentration of 5% (a), TEM images of Cu:ZnInS/ZnS QDs (b, c) and size distribution of Cu:ZnInS/ZnS QDs (d)

The as-prepared QDs appear to be nearly spherical in shape and fairly monodisperse. The average size of Cu:ZnInS/ZnS is about 3.85 nm. The visible lattice fringe indicates that the Cu:ZnInS/ZnS QDs are highly crystalline and the observed lattice spacing is calculated to be 0.32 nm, which matches well to the (1 1 1) plane of ZnS, as shown in Fig. 1(a). The fringe of the QDs is fuzzy, indicating that these QDs are well passivated and protected by OLA.

The PL and UV−Vis spectra of Cu:ZnInS/ZnS QDs synthesized with different Zn/In mole ratios are shown in Fig. 2. The sharp absorption peak of Cu:ZnInS QDs was not observed for the samples with Zn/In mole ratios of 3:1 and 1:1, in contrast to the good resolution of absorption spectra in pure binary QDs. The sample with Zn/In mole ratio of 1:3 shows a sharp absorption peak at 365 nm. With the decrease of Zn/In mole ratio, the UV−Vis spectra present an obvious red shift. The PL spectrum of the as-prepared QDs with Zn/In mole ratio of 1:1 shows the maximum in PL intensity and a broad emission peak at about 550 nm. The big gap between the absorption spectrum and photoluminescence peak demonstrates that emission derives from the Cu-doped emission instead of the intrinsic band gap emission.

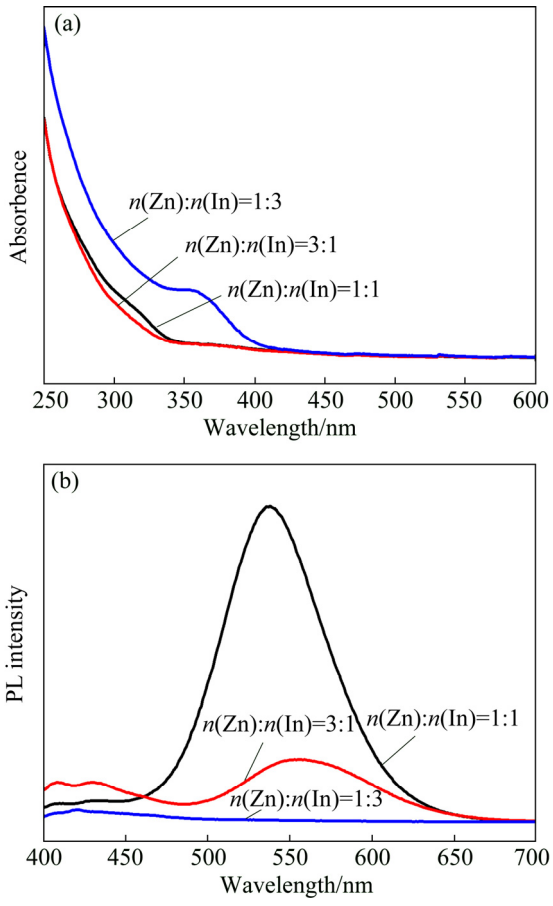

Fig. 2 UV−Vis absorption spectra (a) and PL spectra (b) of Cu:ZnInS/ZnS QDs with Cu concentration of 5% and different Zn/In mole ratios

It has been proved that surface passivation of QDs using suitable inorganic materials with a higher band gap is key to improving the PL efficiency and stability of QDs [25]. Similar attempts for surface passivation of Cu:ZnInS QDs have appeared [26−28], and as expected, good optical properties were obtained. To improve surface passivation, ZnS comprises a near-ideal candidate for construction of core-shell structure around the Cu:ZnInS core, for ZnS exhibits relatively chemical stable and nontoxic characteristics under ambient conditions. The Cu:ZnInS/ZnS core-shell structure was constructed in situ from the Cu:ZnInS QDs. Due to the large excess of sulfur precursor used in the preparation of Cu:ZnInS core QDs, no further sulfur source was added in the process of depositing the ZnS shell. To avoid formation of separate ZnS nanoparticles, Zn precursor was added in batches. Figure 3 shows the PL and UV−Vis spectra of Cu:ZnInS/ZnS QDs with different ZnS shell growth time.

As shown in Figs. 3(b) and (c), the PL peak position blue shifts systematically from the original 554 to 532 nm. The small blue-shift of the PL peak position in the ZnS overcoating process indicates further incorporation of the zinc component into the core material, resulting in an increase of the band gap energy. That is, the blue-shift of PL spectra may be attributed to minor cation exchange between Zn and Cu/In and ZnS shell formation through Zn accumulation on the surface of core QDs following cation exchange [17,18]. It can be seen from Fig. 3(a) that the absorption shoulders of all QD samples are located at similar wavelengths and also present a small blue shift, revealing that the formation of ZnS shell and the cation exchange between Zn and Cu or In.

3.2 Cu, Mn co-doped ZnInS/ZnS core-shell QDs

On the basis of the single-doped Cu:ZnInS/ZnS QDs, we successfully synthesized the Cu,Mn dual-doped ZnInS/ZnS (Cu,Mn:ZnInS/ZnS) core-shell QDs. According to the previous reports, the PL features of doped-dots have a heavy dependence on the dopant concentration. Figure 4 shows the PL spectra of Cu, Mn:ZnInS/ZnS QDs with different Mn concentrations at constant Cu concentration of 5%. The as-synthesized QDs show the tunable emission color from green to orange under ultraviolet excitation. The emission has lower energy than the bandgap of bulk ZnInS. The PL spectra show drastic change in emission bands with the variation of the dopant concentration. With the Mn concentration increasing from 0% to 20%, the original single Cu-doped emission transforms into the tunable dual emission as shown in Fig. 4(a). In order to study this dual emission, peak-differentation-imitating is done for the PL spectra, and the results are shown in Fig. 4(b). The two emission peak positions keep unchanging by

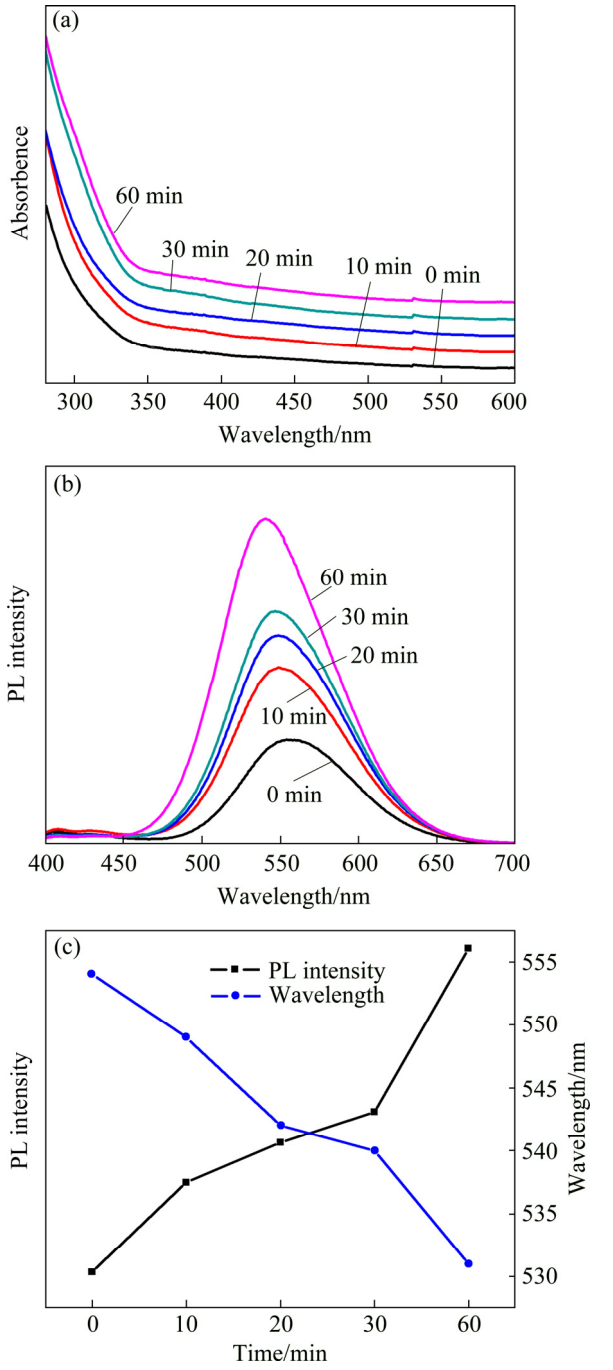

Fig. 3 UV−Vis absorption spectra (a), PL spectra (b) of Cu:ZnInS/ZnS QDs with Cu concentration of 5% under different ZnS shell growth time and dependence of PL intensity and PL peak position on shell growth time (c)

varying the Mn concentrion; however, the relative peak intensity can be tuned with the variation of Mn dopant amount. It is obvious that the two emission peak positions centered at 530 and 585 nm are attributed to the doped-Cu ions and Mn ions, respectively. The emission at 530 nm originates from the energy transition from the conduction band of ZnInS to $^2T_2$ state of Cu, whereas the emission at 585 nm is ascribed to the energy transition from an excited state $^4T_1$ to the ground state $^6A_1$ of Mn.

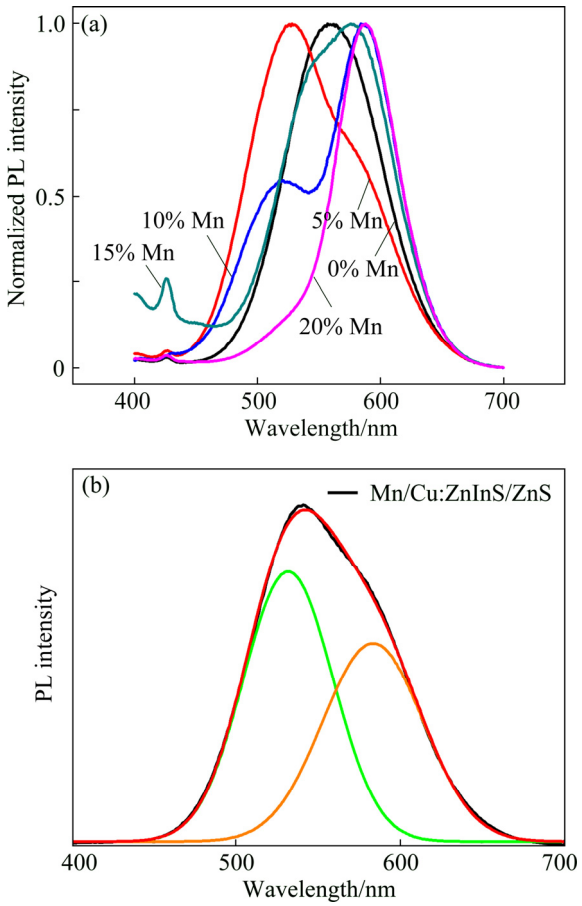

Fig. 4 PL spectra of Cu, Mn:ZnInS/ZnS core-shell QDs with Mn concentrations of 0%, 5%, 10%, 15% and 20% at constant Cu-doping (5%) (a) and peak-differentation-imitating PL spectra (b) with Mn concentration of 5%

Owing to the efficient emission from the dopant luminescence centers, the PL QY of the as-synthesized doped-QDs is relatively high. The PL QY of Cu:ZnInS/ZnS and Cu, Mn:ZnInS/ZnS QDs can respectively reach 49.8% and 30.4%, according to our previous report [24]. In this way, it becomes possible to controll the emission by varying the concentration of the co-doped metal ions. CIE chromaticity coordinate can be calculated from these emission curves by a GoCIE software. Figure 5 shows the CIE color coordinates of the Cu,Mn:ZnInS/ZnS QDs with different Mn concentrtions of 5%, 10%, 0%, 15% and 20%, and the corresponding CIE coordinates are (0.33, 0.53), (0.35, 0.58), (0.40, 0.55), (0.40, 0.50) and (0.50, 0.46), respectively.

3.3 Ag, Mn co-doped ZnInS/ZnS core-shell QDs

The mechanism of Ag-related emission is similar to that of Cu-related emission. Interestingly, the situation is totally different when it comes to Ag, Mn co-doped ZnInS/ZnS (Ag,Mn:ZnInS/ZnS) core-shell QDs. The same method was also used to synthesize Ag, Mn:

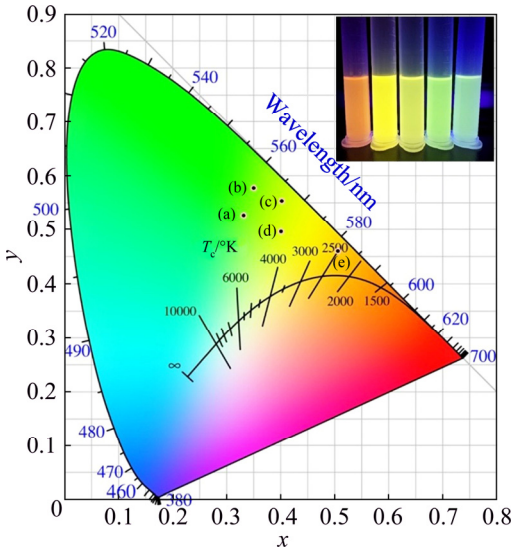

Fig. 5 CIE color coordinates of Cu, Mn:ZnInS/ZnS QDs with Mn concentrtions of 5% (a), 10% (b), 0% (c), 15% (d) and 20% (e) at constant Cu-doping (5%) (Inset is the corresponding digital photograph under UV-light irradiation)

ZnInS/ZnS core-shell QDs, whose PL spectra under different reaction time and Mn/Ag mole ratios are shown in Fig. 6. Instead of showing a dual emission, the PL spectra of Ag, Mn:ZnInS/ZnS QDs in Fig. 6(a) show only a broad peak centered at about 613 nm, which is red-shifted compared with the typical Mn-doped emission peak at 585 nm. It is well-known that the PL of Mn-doped QDs is due to the spin relaxation between its $^4T_1$ and $^6A_1$ states.When excited, the generated exciton in the host transfers its energy to Mn states, which inverts the spins of Mn d^5 electrons. As this is reversed to the ground state, the emission is observed. This red-shift of the emission from 585 to 613 nm is attributed to the interaction of neighboring elements or surface ligands, which affects the Mn ligand-field splitting, thereby decreasing the energy between the Mn d–d states. As shown in Fig. 6(b), the red-shift along with the broadened PL emission from orange to near-red occurs with the incease of the Mn/Ag mole ratio. That is, the PL intensity, peak position and the peak width can be tuned by the variation of the Mn/Ag mole ratio, which can make an important contribution to the white emission.

3.4 Cu, Mn, Ag co-doped ZnInS/ZnS core-shell QDs

Based on the dual-doped QDs, we also synthesized the Cu, Mn, Ag co-doped ZnInS/ZnS (Cu, Mn, Ag:ZnInS/ZnS) core-shell QDs. Figure 7 shows the PL spectra of the as-synthesized QDs under different reaction time. It can be concluded that at the initial stage of QDs growth, the intrinsic emission at 450 nm is dominant. With the increasing reaction time, Mn-doped emission at 585 nm firstly occurs, indicating the easier diffusion of Mn ions into cores than Cu ions, and then

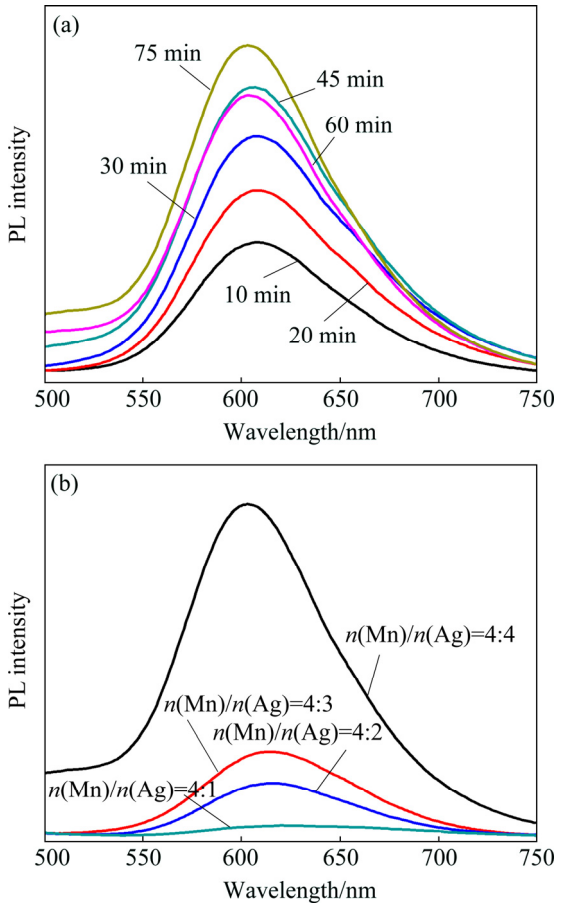

Fig. 6 PL spectra (a) of Ag, Mn:ZnInS/ZnS core-shell QDs with both Ag and Mn concentrations of 5% under different reaction time and PL spectra (b) of Ag, Mn:ZnInS/ZnS core-shell QDs with different Mn/Ag mole ratios at constant Ag-doping (5%)

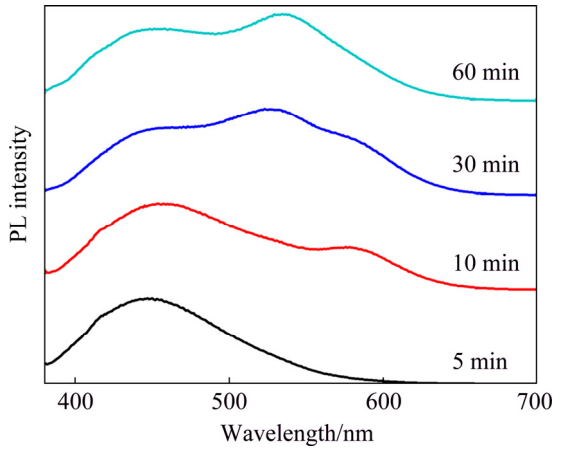

Fig. 7 PL spectra of Ag, Cu, Mn:ZnInS/ZnS QDs with all Ag, Cu and Mn concentrations of 5% under different reaction time

Cu-doped emission at 530 nm occurs and becomes the dominant peak with the further increasing reaction time [24]. It can be expected that the broad emission with three peaks from the Cu, Mn, Ag:ZnInS/ZnS core-shell QDs could make the multi-doped QDs as alternative

materials for white LED applications.

CIE chromaticity coordinate was calculated from the emission curves of all the above doped QD samples by a GoCIE software. Figure 8 shows CIE color coordinates of all the as-prepared doped QDs and the corresponding photographs under a UV lamp. The CIE color coordinates of Cu,Mn:ZnInS/ZnS QDs with different Mn concentrations are located in zone (a), and those of Ag,Mn:ZnInS/ZnS QDs with different Ag/Mn mole ratios are located in zone (b). It can be seen that the tunable emission from green to near-red can be facilely tuned by the variation of the dopant components and concentration. And the quasi-white emission can also be realized from the multi-doped Cu,Mn,Ag:ZnInS/ZnS QDs, whose CIE coordinate is at point (c), and the corresponding coordinate is (0.26, 0.36).

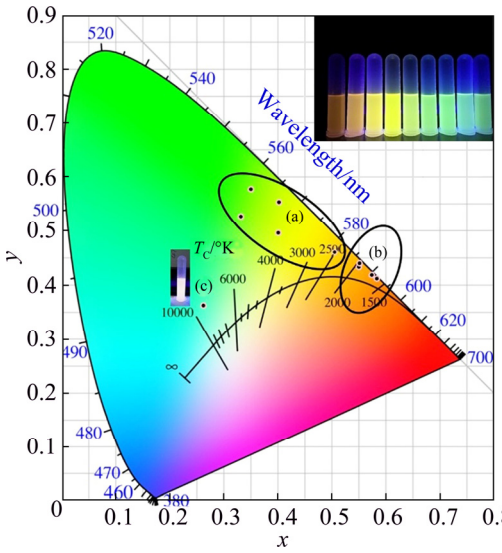

Fig. 8 CIE color coordinates of all as-prepared doped QDs (Inset is the corresponding digital photograph under UV-light irradiation): (a) Cu, Mn:ZnInS/ZnS QDs with different Mn concentrations at constant Cu-doping (5%); (b) Ag, Mn:ZnInS/ZnS QDs with different Ag/Mn mole ratios at constant Ag-doping (5%); (c) Multi-doped Cu, Mn, Ag:ZnInS/ZnS QDs with all Ag, Cu and Mn concentrations of 5%

4 Conclusions

Single-doped, dual-doped and multi-doped ZnInS/ZnS core-shell QDs with the average size of 3.85 nm were successfully synthesized by an optimized one-pot method followed by a hot injection. The as-prepared doped QDs exhibit tunable emission from green to near-red under a single excitation wavelength, which is attributed to the tunable luminescence centers by the variation of the dopant components and concentration. Importantly, quasi-white emission can be achieved from the Cu, Mn, Ag multi-doped ZnInS/ZnS QDs. The primary results demonstrate the promising potential of the doped QDs as alternative materials for white LED applications, and the performance could be further improved by optimizing the synthesis.

References

[1] BROVELLI S, GALLAND C, VISWANATHA R, KLIOV V I. Tuning radiative recombination in Cu-doped nanocrystals via electrochemical control of surface trapping [J]. Nano Letters, 2012, 12(8): 4372−4379.

[2] CHEN H S, WANG S J J, LO C J, CHI J Y. White-light emission from organics-capped ZnSe quantum dots and application in white-light-emitting diodes [J]. Applied Physics Letters, 2005, 86(13): 131905-3.

[3] CHEN H W, ZHU R D, TAN G J, LI M C, LEE S L, WU S T. Enlarging the color gamut of liquid crystal displays with a functional reflective polarizer [J]. Optics Express, 2017, 25(1): 102−111.

[4] JANA S, SRIVASTAVA B B, PRADHAN N. Correlation of dopant states and host bandgap in dual-doped semiconductor nanocrystals [J]. Journal of Physical Chemistry Letters, 2011, 2(14): 1747−1752.

[5] ZHANG W J, ZHOU X G, ZHONG X H. One-pot noninjection synthesis of Cu-doped $Zn_xCd_{1-x}S$ nanocrystals with emission color tunable over entire visible spectrum [J]. Inorganic Chemistry, 2012, 51(6): 3579−3587.

[6] ZHANG W J, LOU Q, JI W Y, ZHAO J L, ZHONG X H. Color-tunable highly bright photoluminescence of cadmium-free Cu-doped Zn−In−S nanocrystals and electroluminescence [J]. Chemistry of Materials, 2014, 26(2): 1204−1212.

[7] SRIVASTAVA B B, JANA S, PRADHAN N. Doping Cu in semiconductor nanocrystals: Some old and some new physical insights [J]. Journal of the American Chemical Society. 2011, 133(4): 1007−1015.

[8] JANA S, SRIVASTAVA B B, PRADHAN N. Correlation of dopant states and host bandgap in dual-doped semiconductor nanocrystals [J]. Journal of Physical Chemistry Letters, 2011, 2(14): 1747−1752.

[9] HE L J, MEI S L, CHEN Q H, ZHANG W L, ZHANG J, ZHU J T, CHEN G P, GUO R Q. Two-step synthesis of highly emissive C/ZnO hybridized quantum dots with a broad visible photoluminescence [J]. Applied Surface Science, 2016, 364: 710−717.

[10] CHEN Y Y, HUANG L J, LI S J, PAN D C. Aqueous synthesis of glutathione-capped Cu^+ and Ag^+-doped $Zn_xCd_{1-x}S$ quantum dots with full color emission [J]. Journal of Materials Chemistry C, 2013, 1(4): 751−756.

[11] CHEN Y Y, LI S J, HUANG L J, PAN D C. Green and facile synthesis of water-soluble Cu−In−S/ZnS core/shell quantum dots [J]. Inorganic Chemistry, 2013, 52(14): 7819−7821.

[12] ZHANG J, CHEN Q H, ZHANG W L, MEI S L, HE L J, ZHU J T, CHEN G P, GUO R Q. Microwave-assisted aqueous synthesis of transition metal ions doped ZnSe/ZnS core/shell quantum dots with tunable white-light emission [J]. Applied Surface Science, 2015, 351: 655−661.

[13] CAO S, ZHAO J L, YANG W Y, LI C M, ZHENG J J. Mn^{2+}-doped Zn−In−S quantum dots with tunable bandgaps and high photoluminescence properties [J]. Journal of Materials Chemistry C, 2015, 3(34): 8844−8851.

[14] YUAN X, MA R X, ZHANG W J, HUA J, MENG XD, ZHONG X H, ZHANG J H, ZHAO J L, LI H B. Dual emissive manganese and copper Co-doped Zn−In−S quantum dots as a single color-converter for high color rendering white-light-emitting diodes [J]. ACS Applied Materials & Interfaces, 2015, 7(16): 8659−8666.

[15] LI J M, LIU Y, HUA J, TIAN L H, ZHAO J L. Photoluminescence properties of transition metal doped Zn−In−S/ZnS core/shell quantum dots in solid films [J]. Rsc Advances, 2016, 6(50): 44859−44864.

[16] ZHANG Q H, TIAN Y, WANG C F, CHEN S. Construction of Ag-doped Zn−In−S quantum dots toward white LEDs and 3D luminescent patterning [J]. RSC Advances, 2016, 6(53): 47616−47622.
[17] ZHANG W J, LOU Q, JI W Y, ZHAO J L, ZHONG X H. Color-tunable highly bright photoluminescence of cadmium-free Cu-doped Zn−In−S nanocrystals and electroluminescence [J]. Chemistry of Materials, 2014, 26(2): 1204−1212.
[18] HUANG G G, WANG C L, XU S H, QI Z Q, LU C G, CUI Y P. Ag- and Mn-doped ZnInS/ZnS dual-emission quantum dots with zone tunability in the color coordinate [J]. Nanotechnology, 2016, 27(18): 185602.
[19] YUAN X, HUA J, ZENG R S, ZHU D H, JI W Y, JING P T, MENG X D, ZHAO J L, LI H B. Efficient white light emitting diodes based on Cu-doped ZnInS/ZnS core/shell quantum dots [J]. Nanotechnology, 2014, 25(43): 435202.
[20] HUANG G G, WANG C L, XU X J, CUI Y P. An optical ratiometric temperature sensor based on dopant-dependent thermal equilibrium in dual emitting Ag&Mn:ZnInS quantum dots [J]. RSC Advances, 2016, 6: 58113−58117.
[21] PRADHAN N. Red-tuned Mn d-d emission in doped semiconductor nanocrystals [J]. ChemPhysChem, 2016, 17(8): 1087−1094.
[22] KE J, LI X Y, ZHAO Q D, SHI Y, CHEN G H. A novel approach to synthesize ultrasmall Cu doped Zn−In−Se nanocrystal emitters in a colloidal system [J]. Nanoscale, 2014, 6(6): 3403−3409.
[23] JANG E, JUN S, JANG H, LLIM J, KIM B, KIM Y. White-light-emitting diodes with quantum dot color converters for display backlights [J]. Advanced Materials, 2010, 22(28): 3076−3080.
[24] ZHU J T, MEI S L, YANG W, ZHANG G L, CHEN Q H, ZHANG W L, GUO R Q. Tunable emission of Cu (Mn)-doped ZnInS quantum dots via dopant interaction [J]. Journal of Colloid and Interface Science, 2017, 506: 27−35.
[25] XIANG W D, YANG H L, LIANG X J, ZHONG J S, WANG J, LUO L, XIE C P. Direct synthesis of highly luminescent Cu−Zn−In−S quaternary nanocrystals with tunable photoluminescence spectra and decay times [J]. Journal of Materials Chemistry C, 2013, 1(10): 2014−2020.
[26] YOON H C, OH J H, KO M, YOO H, DO Y R. Synthesis and characterization of green Zn−Ag−In−S and red Zn−Cu−In−S quantum dots for ultrahigh color quality of down-converted white LEDs [J]. ACS Applied Materials & Interfaces, 2015, 7(13): 7342−7350.
[27] WANG X, LIANG Z R, XU X Q, WANG N, FANG J, WANG J X, XU G. A high efficient photoluminescence Zn−Cu−In−S/ZnS quantum dots with long lifetime [J]. Journal of Alloys and Compounds, 2015, 640: 134−140.
[28] PENG L C, HUANG K K, ZHANG Z L, ZHANG Y, SHI Z, XIE R G, YANG W S. Bandgap- and radial-position-dependent Mn-doped Zn−Cu−In−S/ZnS core/shell nanocrystals [J]. Chem Phys Chem, 2016, 17(5): 752−758.

无镉过渡金属(Cu、Mn、Ag)共掺杂 ZnInS/ZnS 核壳结构量子点的可调谐发光

陈秋行，梅时良，杨 武，张万路，张桂林，朱嘉弢，郭睿倩

复旦大学 先进照明技术教育部工程研究中心 电光源研究所，上海 200433

摘 要：通过简易环保的方法合成一种以过渡金属(Cu、Mn 和 Ag)掺杂 ZnInS 为内核、ZnS 为壳层的发光可调谐的核壳结构量子点(平均粒径 3.85 nm)。在油相体系中，以十二硫醇(DDT)和油胺(OLA)为稳定剂，通过一锅法先在体系中形成内核量子点，随后通过热注射法包覆 ZnS 壳层。在量子点的合成中，引入过渡金属(Cu、Mn 和 Ag)进行单独掺杂或共掺杂，实现量子点的可调谐发光。通过调节掺杂元素的种类、掺杂浓度以及前驱体 Zn/In 的比例，所合成的量子点发光可以在绿光(530 nm)到近红光(613 nm)范围内进行调节。通过 3 种过渡金属(Cu、Mn 和 Ag)的共掺杂，成功获得具有准白光发射的量子点。结果表明，这种共掺杂量子点在未来高性能白光 LED 应用领域有很好的发展前景。

关键词：Zn 族量子点；核壳结构；掺杂；可调谐发光；白光

(Edited by Xiang-qun LI)